Synthesis of a Carbene-Stabilized (Diphospha)aminyl Radical and its One Electron Oxidation and Reduction to Nonclassical Nitrenium and Amide Species

Etienne A. LaPierre,[1] Lara K. Wantanabe,[2] Brian O. Patrick,[3] Jeremy M. Rawson,[2] Heikki M. Tuononen,*[4] and Ian Manners*[1]

[1]Department of Chemistry, University of Victoria, 3800 Finnerty Rd, Victoria, British Columbia, V8P 5C2, Canada

[2] Department of Chemistry and Biochemistry, University of Windsor, 401 Sunset Avenue, Windsor, Ontario N9B 3P4, Canada

[3]Department of Chemistry, University of British Columbia, 2036 Main Mall, Vancouver, British Columbia, V6T 1Z1, Canada

[4] Department of Chemistry, NanoScience Centre, University of Jyväskylä, P.O. Box 35, FI-40014 Jyväskylä, Finland

ABSTRACT: Herein we report the synthesis of the acyclic carbene-stabilized diphospha(aminyl) radical $CAAC^{Me}PNPCAAC^{Me}$ **4** ($CAAC^{Me}$=1-[2,6-bis(isopropyl)phenyl]-3,3,5,5-tetramethyl-2-pyrrolidinylidene) by a facile one-pot, 7-electron reduction of hexachlorophosphazene chloride $[Cl_3PNPCl_3][Cl]$. The PNP radical **4** features a conjugated framework with spin density primarily localized on the central nitrogen atom as well as the flanking carbenes. Unlike other tripnictogen radicals, **4** undergoes facile one-electron oxidation and reduction to yield non-classical nitrenium and amide species $[\mathbf{5}]^+$ and $[\mathbf{6}]^-$, respectively. The cation $[\mathbf{5}]^+$ exhibits conformational flexibility in the solution state between the expected W-shaped geometry $[\mathbf{5_b}]^+$ and a previously unobserved linear heteroallene type structure $[\mathbf{5_a}]^+$, which was characterized in the solid state. The equilibrium was explored both computationally and experimentally, showing that $[\mathbf{5_a}]^+$ is favored over $[\mathbf{5_b}]^+$ both enthalpically ($\Delta H = -2.9 \times 10^3 \pm 80$ J mol^{-1}) and entropically ($\Delta S = 4.2 \pm 0.25$ J mol^{-1} K^{-1}). The formal amide $[\mathbf{6}]^-$ displays remarkable flexibility in its coordination chemistry, due to the presence of multiple Lewis basic centers, as evidenced by the structure of its potassium complex $\mathbf{K_2 6_2}$, which exhibits both μ,κ-P,κ-P and η^3-PNP coordination modes. Protonation of $[\mathbf{6}]^-$ leads to the formation of an amine **7**, which features a trigonal planar geometry around nitrogen.

Introduction

The design of stable nitrogen radicals is a longstanding challenge in synthetic chemistry.[1-3] Acyclic aminyl radicals of the type NRR′ remain particularly elusive, despite being implicated as critical intermediates in a variety of chemical transformations of synthetic organic or biological importance,[3-7] as well as their potential utility in polymer synthesis and materials applications.[8-9] Accordingly, few structurally characterized examples of these compounds have been realized.[10-19] One major hurdle in the development of this chemistry is the lack of well-defined synthetic methodologies. An increasingly popular strategy for the generation of isolable *p*-block radical species is the reduction of main-group halides or pseudo-halides in the presence of, or ligated by, stable carbenes, *e.g. N*-heterocyclic (NHCs) or cyclic alkylamino carbenes (CAACs), leading to the formation of the carbene-stabilized radical species.[20-23] Unfortunately, the instability of binary nitrogen halides precludes their use in synthesis,[24] rendering the use of strategies employed for other *p*-block elements impractical. While other nitrogen sources, such as azides and arylimidazolium dyes,[16-17, 25-28] have been successfully used in the generation of carbene-stabilized nitrogen radicals (Chart 1), this field remains under-developed compared to that of related *p*-block elements, such as phosphorus,[29-32] and the development of additional nitrogen synthons is highly desirable.

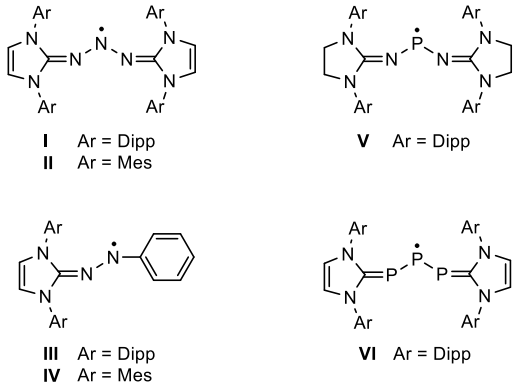

Chart 1. Select carbene-stabilized nitrogen and phosphorus radicals.

Potential candidates for the generation of nitrogen radicals using reductive approaches are halophosphazenes *P*-trichloro-*N*-trimethylsilyl-phosphoranimine (Cl_3P=NTMS) and hexachlorophosphazene chloride ([Cl_3PNPCl_3][Cl]). These long-known compounds are readily accessible on gram scale[33-36] and have been extensively used in the synthesis of chlorophosphazene rings and polymers,[33, 37-41] although little is known about their reduction chemistry.[42] Exhaustive reduction of these materials should provide a convenient route to binary PN molecules, an elusive class of compounds of longstanding interest as inorganic analogues of archetypal hydrocarbons,[43-44] energetic materials,[45-49] and components of interstellar media.[50-53] Further, the presence of terminal chlorophosphorane moieties should allow for facile extension of well-explored carbene-phosphorus chemistry[23, 29, 54-62] to a formally nitrogen-based system. With these considerations in mind, we have explored the reactivity of Cl_3P=NTMS and [Cl_3PNPCl_3][Cl] with cyclic alkylamino carbene 1-[2,6-bis(isopropyl)phenyl]-3,3,5,5-tetramethyl-2-pyrrolidinylidene ($CAAC^{Me}$).

Results and Discussion

1. Synthesis and Characterization of **1**, **2**, and [**3**]$^+$

We first attempted the construction of the PNP core in a stepwise fashion by treating *P*-trichloro-*N*-trimethylsilyl-phosphoranimine[36, 63] with 2 eq. of $CAAC^{Me}$, which effected both reduction and simultaneous ligation of the generated highly reactive *P*-chloro-*N*-trimethylsilyl-iminophosphine, a proposed, but never observed, intermediate in the phosphine-mediated dehalogenation of this phosphoranimine.[64-65] The resulting thermally-sensitive adduct **1** can be readily isolated from the by-product [$CAAC^{Me}$-Cl][Cl] (*vide infra*) by filtration and isolated as pure, red crystalline solid in 74% yield. Compound **1** was characterized by multinuclear NMR spectrometry (Figures S18-S20) and single crystal X-ray diffraction (Figure 1). Treatment of **1** with excess PCl_3 completed the PNP core, leading to a single product as observed by $^{31}P\{^1H\}$ NMR spectrometry with two resonances integrating 1:1 at 176.2 and 109.5 ppm (Figure S22). These data were assigned to the $CAAC^{Me}$-stabilized *P*-chloro-*N*-dichlorophosphino-iminophosphine **2** based on its solid-state structure (Figure 1) and mass spectrum (M^+ = 466.10 amu, $\{M-Cl\}^+$ = 431.13 amu, Figure S1).

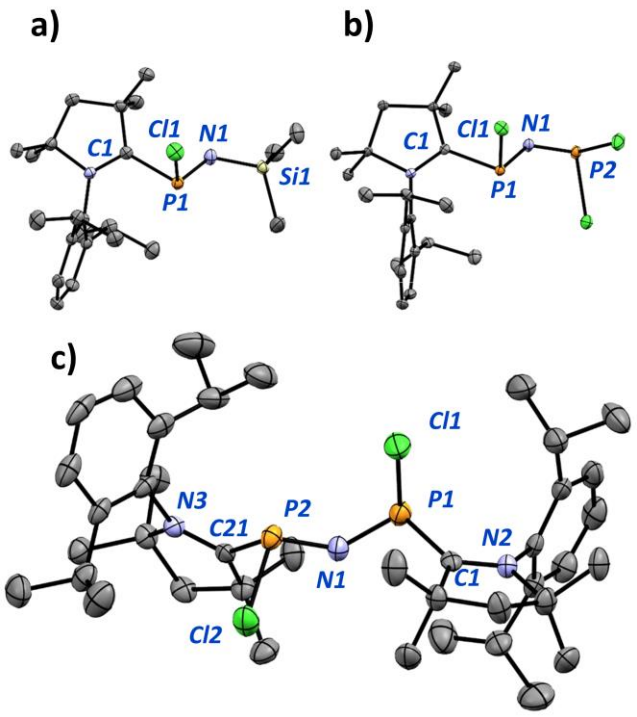

Figure 1. Molecular structure of **1** (a), **2** (b) and [**3**]$^{+}$ (c). Ellipsoids are drawn at 50% probability. Only one crystallographically independent molecule of **1** is shown. Hydrogen atoms and the counter anion in the structure of [**3**][Cl] are omitted for clarity. Select bond lengths (Å) and angles (°) for **1**: C1-P1 1.906(1); N1-P1 1.569(1); N1-Si1 1.700(1); P1-Cl1 2.2924(5); N2-C1 1.299(2) C1-P1-Cl 86.59(4); P1-N1-Si1 128.99(8). Select bond lengths (Å) and angles (°) for **2**: C1-P1 1.891(1); N1-P1 1.625(2); N1-P2 1.584(1); P1-Cl1 2.1296(7); C1-N2 1.296(2) C1-P1-Cl 90.74(1); P1-N1-P2 132.5(1). Select bond lengths (Å) and angles (°) for **3** [calculated values in square brackets]: C1-P1 1.905(2) [1.897]; C21-P2 1.898(3) [1.878]; N1-P1 1.591(3) [1.604]; N1-P2 1.599(3) [1.604]; P1-Cl1 2.149(2) [2.136]; P2-Cl2 2.130(1) [2.158]; C1-N2 1.289(4) [1.291]; N2-C21 1.294(3) [1.291]; P1-N1-P2 137.1(2) [133.3].

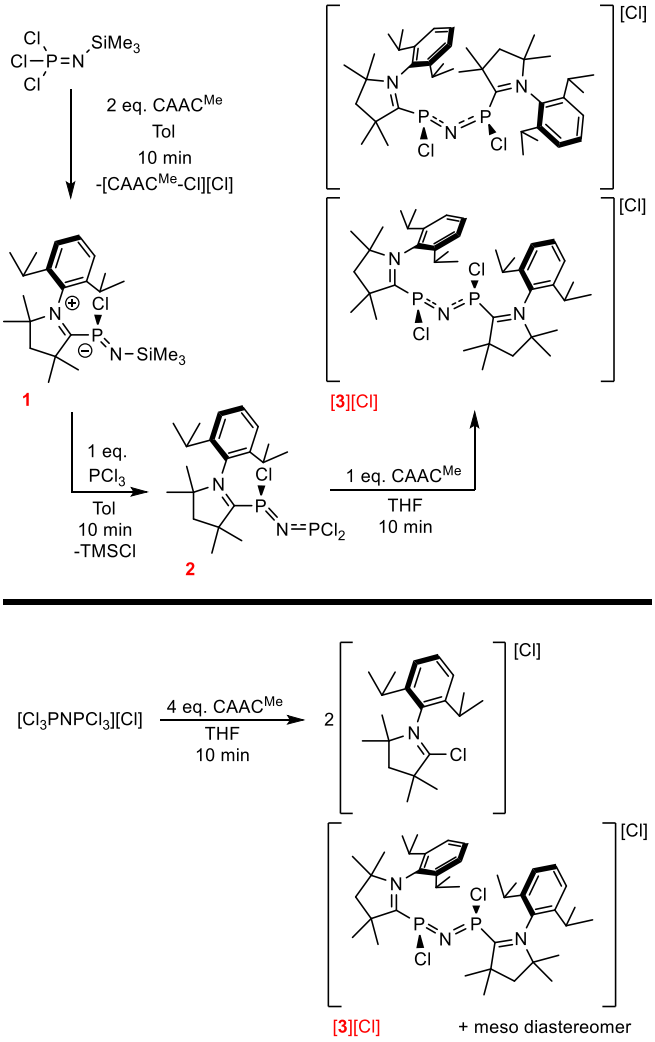

Scheme 1. Synthesis of compounds **1**, **2**, and [**3**][Cl].

Addition of 1 eq. of $CAAC^{Me}$ to a THF solution of **2** led to rapid precipitation of brown-yellow crystals. Dissolution of the precipitate in CD_2Cl_2 and subsequent NMR spectrometric analysis revealed the presence of two $^{31}P\{^1H\}$ resonances at 141.6 and 108.1 ppm in a ca. 1:2 ratio (Figure S24), while the ^1H NMR spectrum is indicative of two $CAAC^{Me}$-containing complexes (Figure S23). Both species show a loss of mirror symmetry in the $CAAC^{Me}$ moiety on the NMR timescale as evidenced by the doubling of all resonances, except those corresponding to the aryl *para*-H, and the splitting of the resonances of ring methylene protons into characteristic AB doublet of doublets, suggestive of low symmetry. Single crystal X-ray diffraction studies revealed the formation of [**3**][Cl] (Figure 1) in which the cation $[\mathbf{3}]^+$ is present as a racemate. This suggests that the minor species observed in the solution is the *meso* diastereomer of $[\mathbf{3}]^+$ (Scheme 1). The single phosphorus and carbene environments observed by NMR for both species can be explained by rapid inversion at nitrogen in solution that is distinctive to phosphazene cations.[66] Accordingly, DFT (see SI for full computational details) calculations performed on $[\mathbf{3}]^+$ showed the barrier ($\Delta G^{\ddagger}$) for nitrogen inversion to be only 19 kJ mol^{-1}. The metrical parameters of **1**, **2**, and $[\mathbf{3}]^+$ are similar to *N*-heterocyclic carbene adducts of stable iminophosphines reported by Burford and coworkers,[67-68] and include unusually small $C_{carbene}$-P-Cl angles (*ca.* 90°) along with long $C_{carbene}$-P (*ca.* 1.90 Å) and short $C_{carbene}$-N (*ca.* 1.29 Å) and N-P (*ca.* 1.59 Å) bond lengths indicative of single and multiple bond character, respectively, as drawn in Scheme 1.[69] Formally, [**3**][Cl] can be viewed as the biscarbene adduct of the heteroallene salt [ClPNPCl][Cl]. The cation can be described with resonance structures [Cl–P^+–N=P–Cl] ↔ [Cl–P=N–P^+–Cl] in which the empty *p*-orbital on the phosphorous atom (one on each structure) is perfectly poised to accept an electron pair from $CAAC^{Me}$. This is also borne out by DFT calculations on $[ClPNPCl]^+$ that show the LUMO and LUMO+1 to be linear combinations of *p*-orbitals with the greatest contributions from the two phosphorus atoms.

In an attempt to develop a more expedient route to [**3**][Cl], the reaction of $[Cl_3PNPCl_3][Cl]$ with 4 eq. (or more) of $CAAC^{Me}$ in THF solution was found to lead to rapid formation of a colorless solution over a yellow precipitate. Dissolution of the precipitate in CD_2Cl_2 and subsequent NMR analysis revealed the presence of two $^{31}P\{^1H\}$ resonances (δ_P = 141.6, 108.1) in a *ca.* 1:2 ratio (Figure S2), corresponding to $[\mathbf{3}]^+$, while the ^1H NMR spectrum is consistent with the formation of three $CAAC^{Me}$ containing compounds in an approximately 6:2:1 ratio (Figure S3). The latter two resonances match the spectrum for $[\mathbf{3}]^+$, while the most intense one is consistent with the formation of 2 eq. of the 2-chloropyrrolium salt $[CAAC^{Me}\text{-Cl}][Cl]$,[59, 70] which was confirmed by independent synthesis (Figure S4; see SI for full synthetic details). This suggests that 2 eq. of $CAAC^{Me}$ effected the $4e^-$ reduction of $[Cl_3PNPCl_3][Cl]$. Unfortunately, the similar solubilities of $[CAAC^{Me}\text{-Cl}][Cl]$ and $[\mathbf{3}]^+$ prevented their isolation or separation from the mixture. Nevertheless, the expedient one-step synthesis of this mixture proved to be advantageous for further synthetic work as $[CAAC^{Me}\text{-Cl}][Cl]$ could be removed after additional reactions.

2. Reduction of $[\mathbf{3}]^+$ to Radical **4**

Attempts to reduce either isolated [**3**][Cl] or [**3**][Cl] generated *in situ* from the reaction of $[Cl_3PNPCl_3][Cl]$ with $CAAC^{Me}$ with commonly used strong reducing agents, such as magnesium or potassium, resulted in mixtures of diamagnetic species by ^{31}P NMR spectrometry. However, the use of 1.5 eq. of mild, salt-free, reducing agent 1,4-bis(trimethylsilyl)dihydropyrazine (TMS-DHP)[71-73] with isolated or freshly generated suspensions of [**3**][Cl] in THF resulted in the immediate formation of a dark pink solution over a white precipitate (Scheme 2). Filtration and removal of volatiles afforded the radical **4** as a dark pink solid in 81% yield, the identity of which was confirmed by mass spectrometry (M+H = 647.45 amu, Figure S6), solution magnetic moment (Evans method, μ_{eff} = 1.78 μ_B),[74] single crystal X-ray diffraction (Figure 2), and EPR spectrometry (Figure 3).

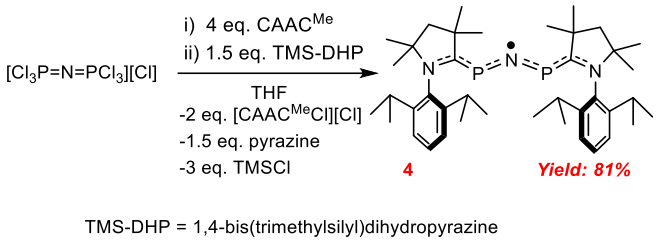

Scheme 2. Synthesis of carbene-stabilized PNP radical **4**.

Radical **4** is stable at ambient temperature for months as a solid in tightly sealed vials under an inert atmosphere and at least one week in C_6D_6 solution; however, heating C_6D_6 solutions to 80 °C for 48 h leads to the formation multiple unidentified diamagnetic phosphorus species by $^{31}P\{^1H\}$ NMR spectrometry, while exposure to oxygen results in immediate loss of the characteristic pink color and degradation. Furthermore, **4** does not react with H-atom transfer reagents 9,10-dihydroanthracene or xanthene, unlike related NHC-stabilized triazenyl radicals **I** and **II** (Chart 1),[17] suggesting an N-H bond strength for the corresponding amine (*vide infra*) of less than 315 kJ mol^{-1}. [75-76]

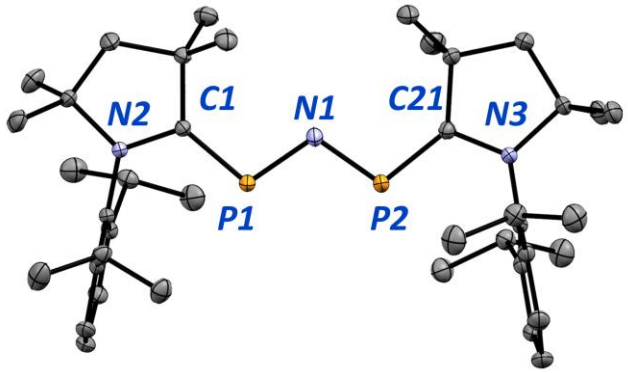

Figure 2. Molecular structure of **4**. Ellipsoids are drawn at 50% probability. Hydrogen atoms are omitted for clarity. Select bond lengths (Å) and angles (°) for **4** [calculated values in square brackets]: N1-P1 1.667(1) [1.651]; N1-P2 1.660(1) [1.651]; C1-P1 1.738(1) [1.736]; C21-P2 1.743(1) [1.736]; C1-N2 1.367(1) [1.358]; C21-N3 1.366(1) [1.358]; P1-N1-P2 110.75(6) [114.4].

The UV-VIS absorption spectrum of **4** in THF consists of a strong, broad peak with λ_{max} = 550 nm ($\varepsilon = 1.7\times10^4$ M^{-1} cm^{-1}) as well as two less intense absorbtions at *ca.* 700 nm ($\varepsilon = 1.0\times10^3$ M^{-1} cm^{-1}) and 340 nm ($\varepsilon = 2.7\times10^3$ M^{-1} cm^{-1}) (Figure S7). The solid-state structure of **4** is characterized by a nearly planar orientation of the central PNP fragment and $CAAC^{Me}$ ligands, with metrical parameters indicative of multiple bond character and extensive delocalization throughout the PNP-carbene framework (Figure 2).[69] The EPR spectrum of **4** in toluene solution at 298 K reveals a 13-line multiplet (Figure 3) that could be successfully simulated with g_{iso} = 2.004 and hyperfine coupling to the central nitrogen atom (a_N = 5.99 G) as well as to both phosphorus (2 × a_P = 6.20 G) and carbene nitrogen atoms (2 × a_N = 3.05 G).

DFT calculations well reproduce the W-shape geometry of **4** with a nearly planar CPNPC unit (Figure 2). The singly occupied molecular orbital (SOMO) of **4** is of π-type and $C_{carbene}$-P bonding and N-$C_{carbene}$ and N-P anti-bonding (Figure 4), resembling the SOMOs of NHC-stabilized triazenyl radicals **I** and **II** (Chart 1). The calculated spin density of **4** mirrors the shape of the SOMO (Figure 4), with additional β-spin contributions on phosphorus atoms that arise from spin polarization effects. As is evident from the shape of the SOMO and the associated population analyses, only around 35% of α-spin density resides on the central nitrogen atom in **4**, with the remainder spread over the $C_{carbene}$ and N atoms on the two $CAAC^{Me}$ ligands. Thus, **4** is only formally a nitrogen-centered radical and its lack of reactivity with common H-atom transfer reagents is consistent with the calculated N-H bond enthalpy of 274 kJ mol^{-1} at 298 K for the corresponding amine in the gas phase. The calculated hyperfine coupling constants for **4** show coupling to all three nitrogen atoms, 4.70 and 2 × 2.42 G, in good agreement with the values from spectral simulation. However, at 2 × −15.1 G, the calculations significantly overestimate the spin-polarization induced phosphorus couplings.

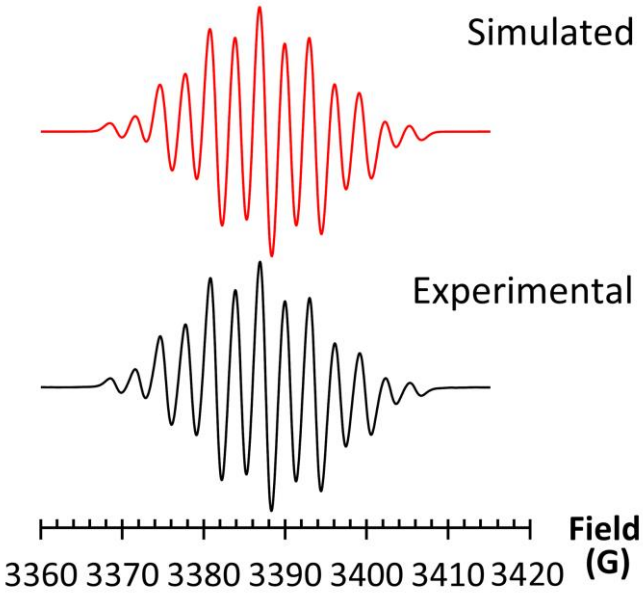

Figure 3. Simulated and experimental (in toluene at 298 K) EPR spectrum of **4**.

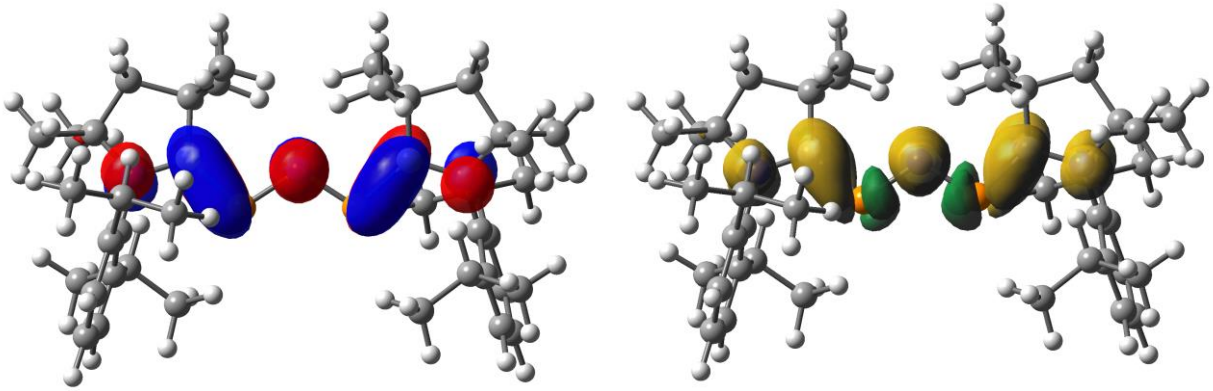

Figure 4. Calculated SOMO (left, isosurface value 0.04) and spin density (right, isosurface value 0.002) of **4**.

Because the synthesis of related carbene stabilized triazenyl and triphosphorus radicals was accomplished by one-electron reduction of the corresponding azido and phosphonium cations,[17, 25, 31] and owing to the growing importance of cationic nitrenium species as potential organocatalysts and ligands,[19, 77-83] the ability of **4** to act as a precursor to a phosphorus-stabilized nitrenium cation was explored. The cyclic voltammogram of **4** in THF (Figure 5) revealed both the anticipated reversible oxidation wave ($E_{1/2}^{ox}$ = –1.09 *vs*. Fc/Fc$^+$), which occurs at a significantly more positive potential than that reported for the triazyl radicals **I** and **II** (*cf.* $E_{1/2}^{ox}$ = –1.17/–1.38 V *vs*. Ag/AgCl in THF,[17] *ca.* –1.76/–1.97 *vs.* Fc/Fc$^+$)[84-86] and a partially reversible reduction event ($E_{1/2}^{red}$ = –2.08 vs. Fc/Fc$^+$), which has not been previously observed for related compounds (Chart 1). Accordingly, both the chemical one-electron oxidation and reduction of **4** were investigated.

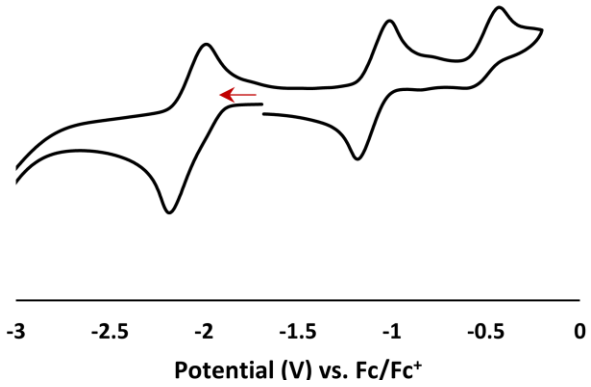

Figure 5. Cyclic voltammogram of **4** (in THF, 0.1 M [*n*-Bu$_4$N][PF$_6$], ~1 mM analyte, 100 mV s^{-1} scan rate, Pt working electrode).

3. Chemical Oxidation of **4** to [**5**]$^{+}$

Treatment of **4** with one equivalent of the mild oxidant [CPh_3][SbF_6] in DCM resulted in an immediate color change from pink to blue-purple, from which a dark blue microcrystalline solid [**5**][SbF_6] could be isolated in excellent yield (Scheme 3). Analysis of the material by $^{31}P\{^{1}H\}$ NMR spectrometry revealed the presence of two resonances at 269.6 ppm and 185.1 ppm in a *ca.* 1:5.5 ratio (Figure S8), while the ^{1}H NMR spectrum at 298 K shows two sets of broadened peaks indicative of dynamic exchange (Figure S9), which was further supported by the presence of negatively phased off-diagonal peaks in the 2D-EXSY ^{1}H NMR spectrum (Figure S10). Variable temperature ^{1}H NMR spectrometry shows a sharpening of both sets of resonances at lower temperatures (Figure S9).

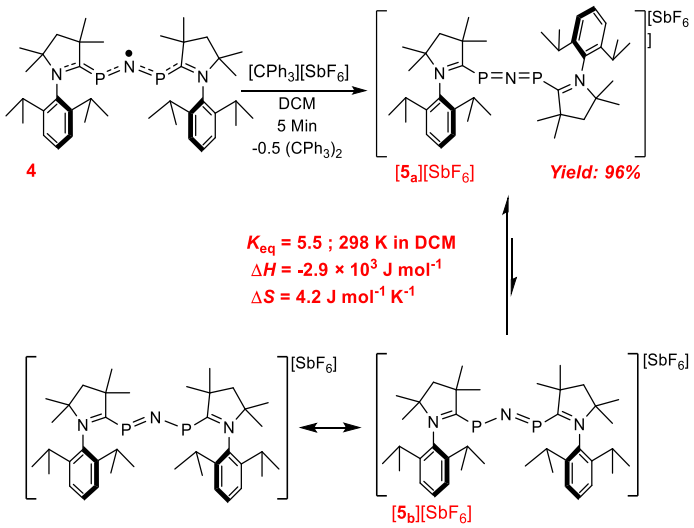

Scheme 3. Oxidation of **4** to [**5**]$^{+}$ and equilibrium between [**5**$_a$]$^{+}$and [**5**$_b$]$^{+}$

Analysis of the solid-state structure of [**5**]$^+$ by single crystal X-ray diffraction studies revealed not the expected bent W-shaped cation previously reported for related azido and phosphonium salts,[17, 25, 31, 87] but a heteroallene type structure (Figure 6) featuring a nearly linear central PNP unit (175.8(2)°) and C-P (1.826(2) and 1.842(2) Å) and N-P bond lengths (1.581(2) and 1.589(2) Å) suggestive of single and multiple bonding.[69] DFT calculations (PBE1PBE-D3/def2TZVP) indicated that both linear ([**5**$_\mathbf{a}$]$^+$) and W-shaped ([**5**$_\mathbf{b}$]$^+$) geometries are stable minima on the potential energy surface in the gas phase, with [**5**$_\mathbf{a}$]$^+$ favored by –11 and –18 kJ mol^{-1} in enthalpy and Gibbs energy at 298 K. The calculated chemical shifts of [**5**$_\mathbf{a}$]$^+$and [**5**$_\mathbf{b}$]$^+$ are 163.9 and 261.2 ppm, respectively, and in reasonable agreement with the NMR data of [**5**]$^+$ in solution (*vide supra*). Van't Hoff analysis of the equilibrium in CD_2Cl_2 (Figure S11) showed that [**5**$_\mathbf{a}$]$^+$ is slightly favored over [**5**$_\mathbf{b}$]$^+$ both in enthalpy ($\Delta H = -2.9\times10^3 \pm 80$ J mol^{-1}) and in entropy ($\Delta S = 4.2 \pm 0.25$ J mol^{-1} K^{-1}), giving $\Delta G = -4.2$ kJ mol^{-1} at 298 K.

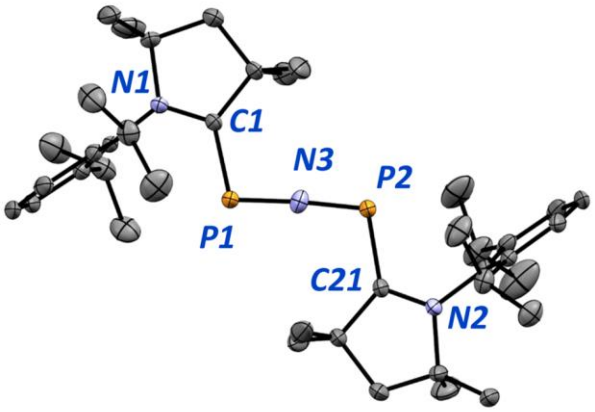

Figure 6. Molecular structure of [**5**$_\mathbf{a}$]$^+$. Ellipsoids are drawn at 50% probability. Hydrogen atoms and counterion are omitted for clarity. Select bond lengths (Å) and angles (°) for [**5a**]$^+$ [calculated values in square brackets]: N3-P1 1.589(2) [1.585]; N3-P2 1.581(2) [1.585]; C1-P1 1.826(2) [1.825]; C21-P1 1.842(2) [1.825]; C1-N1 1.308(3) [1.306]; C21-N2 1.306(3) [1.306]; P1-N1-P2 175.8(2) [180.0]; C1-P1-N3 103.9(1) [103.5].

The structural dichotomy observed for [**5**]$^+$ is reminiscent of that known for the bis(triphenylphosphine)iminium cation,[66] [Ph_3PNPPh_3]$^+$, whose PNP moiety has a very shallow bending potential and can adopt either bent or linear geometry in the solid state, though only the bent form is a stable minimum on the potential energy surface. Examination of the calculated structures for [**5**$_\mathbf{a}$]$^+$ and [**5**$_\mathbf{b}$]$^+$ shows that the key bond parameters are not significantly affected by the PNP angle, with only very minor differences (less than 0.05 Å) observed in the key N-P, $C_{carbene}$-P and $C_{carbene}$-N distances. Formally, [**5**]$^+$ can be viewed as the biscarbene adduct of the linear [PNP]$^+$ cation, with electron donation primarily from CAAC^{Me} to [PNP]$^+$. Natural population and bond orbital analyses conducted for [**5**$_\mathbf{a}$]$^+$ indicate a slightly positively charged PNP fragment (partial charges of +0.77 and −1.25 e on N and P, respectively) in which the N atom is *sp*-hybridized with one *p*-orbital engaging in π-type bonding interactions with the P atoms (a 3c-4e hyperbonded PNP triad) and the other one holding a lone pair of electrons (Figure S39). Second-order perturbative estimates of donor-acceptor interactions show that the electrons in the PNP unit are highly delocalized, indicating that an idealized single Lewis structure description of bonding is inadequate (also applies to **4** and [**6**]$^-$, *vide infra*). The charge distribution (partial charges of +0.77 and −1.15 e on N and P, respectively) and NBO description of [**5**$_\mathbf{b}$]$^+$ is similar to [**5**$_\mathbf{a}$]$^+$ but the N atom is sp^2-hybridized, consistent with the bent PNP angle. Electron localization function (ELF) analyses performed for [**5**]$^+$ show a similar picture (Figure S40). In [**5**$_\mathbf{a}$]$^+$, the central N atom is surrounded by two monosynaptic V(N) and two disynaptic V(N,P) basins with average populations of 2 × 1.93 and 2 × 1.70 e$^-$, respectively, whereas [**5**$_\mathbf{b}$]$^+$ shows one monosynaptic V(N) and two disynaptic V(N,P) basins with populations of 2.59 and 2 × 2.28 e$^-$, respectively. The standard deviations and relative fluctuations associated with these basins are all rather high, indicating correlation between basin populations and, thereby, high degree of delocalization.

4. Chemical Reduction of **4** to [**6**]$^{-}$

Given the unanticipated results observed in the oxidation chemistry of **4** and the presence of a partially reversible reduction wave in its cyclic voltammogram, the chemical reduction of **4** was also pursued. Treatment of either THF or aromatic hydrocarbon solutions of **4** with one or more equivalents of KC_8 led to the formation of a deep red-orange solution, which contains resonances for one major product **K6$_{sol}$** (> 92–98 %) in the $^{31}P\{^1H\}$ NMR spectrum (Figure S28) with a highly solvent dependent chemical shift (δ_P = 185.9 (THF-d_8), 177.4 (Tol-d_8) and 172.0 (C_6D_6)), as well as an additional peak at 130.4 ppm (Tol-d_8) corresponding to byproduct **7** (*vide infra*) and representing the balance of the phosphorus content. The ^1H NMR spectra in all solvents examined are consistent with one major CAAC^{Me} containing product of apparent C_{2v} symmetry (Figure S29), though the resonances in THF are significantly broadened. Further, the molecular weight of **K6$_{sol}$** in toluene solution was determined by ^1H-DOSY NMR spectrometry (Figure S12) using the external calibration curve method[88] to be 783 Da, which is in excellent agreement with the formulation of **K6$_{sol}$** in toluene as a monomeric potassium amide monosolvate (calculated value 778 Da), although the exact solution structure is unclear.

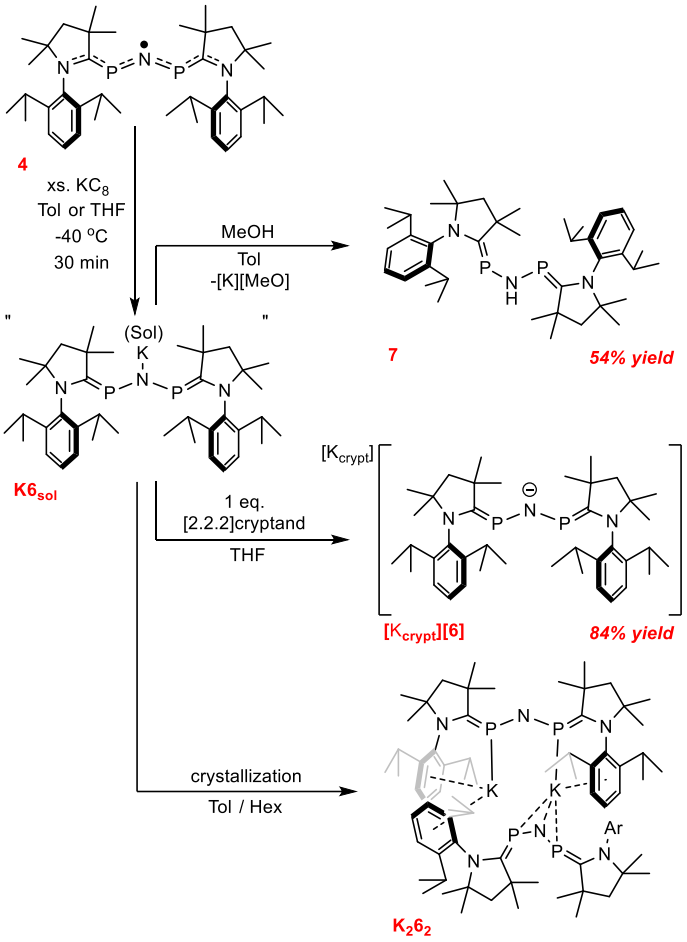

Scheme 4. Reduction of **4** to **K6$_{sol}$** and subsequent reactivity.

All attempts to isolate the species by solvent removal led to an increase in the amount of a diamagnetic phosphorus byproduct **7** characterized by a peak in the $^{31}P\{^{1}H\}$ NMR spectrum at 130.4 ppm (Tol-d_8), which splits into a doublet (J = 4 Hz) in the ^{31}P NMR spectrum, suggestive of nitrogen-centered protonation, despite rigorously anhydrous conditions. Correspondingly, treatment of a freshly prepared toluene solution of **K6$_{sol}$** with excess dry, degassed methanol leads to immediate formation of a bright yellow solution, from which a bright yellow solid can be isolated in 54 % overall yield from **4**. The ^{31}P NMR spectrum of the isolated material reveals **7** to be the major component (*ca.* 96 %, Figures S13 and S14) while the ^{1}H NMR spectrum shows a broad triplet peak at 1.67 ppm integrating to one proton relative to peaks for the CAAC^{Me} moieties (Figure S15). Further, the observed coupling constant matches that of **7** in the ^{31}P NMR spectrum and correlation was observed in the ^{1}H–^{31}P NMR HMBC NMR spectrum, consistent with formulation of **7** as an amine. Nitrogen-centered protonation was further supported by determination of the solid-state structure of **7** by single crystal X-ray diffraction (Figure 7).

The structure of **7** (Figure 7) shows a trigonal planar geometry ($\Sigma_{\angle N}$= 359°) around nitrogen, suggesting sp^2 hybridization. However, at 1.732(4) and 1.719(3) Å, the two N-P bonds are indicative of single bond character, while the two C-P bonds, 1.735(3) and 1.742(5) Å, are clearly of multiple bond character.[69] The bonding in **7** can be understood by considering its formation *via* reduction of [**5**]$^+$ to [**6**]$^-$ through **4**, followed by protonation at nitrogen. The reduction introduces two electrons to the π-type LUMO of [**5**]$^+$, *i.e.*, the SOMO of **4** (Figure 4), that is $C_{carbene}$-P bonding and N-P anti-bonding; the π-type P-N-P bonding orbital is significantly lower in energy and doubly occupied in [**5**]$^+$, **4**, and [**6**]$^-$. Thus, the C-P and N-P bonds in [**6**]$^-$ are short and long, respectively, and the central nitrogen atom is highly electron rich and, thereby, susceptible to protonation. The structure of [**6**]$^-$ (*vide infra*) is in good agreement with this description and further shows that the carbon atoms of the two CAAC^{Me} ligands are twisted by *ca.* 20° from the plane defined by the central PNP fragment. This is significantly less than in **7** in which the ligands are almost perpendicular to the PNP plane, presumably to alleviate repulsion between the N-H proton and the substituents on the carbene moiety. As the PNP fragment is better at delocalizing electron density than an NNN unit in **I**, the geometry around the central nitrogen atom is **7** is planar, not pyramidal, complemented with increased phosphinidene character at the P atoms. Calculations probing the possible reactivity of **7** as a hydrogen atom donor (*vide supra*) showed that the transformation **7** → **4** + ½ H_2 has a positive reaction enthalpy of 68 kJ mol^{-1} at 298 K in the gas phase, in agreement with experimental observations of the stability of **7**.

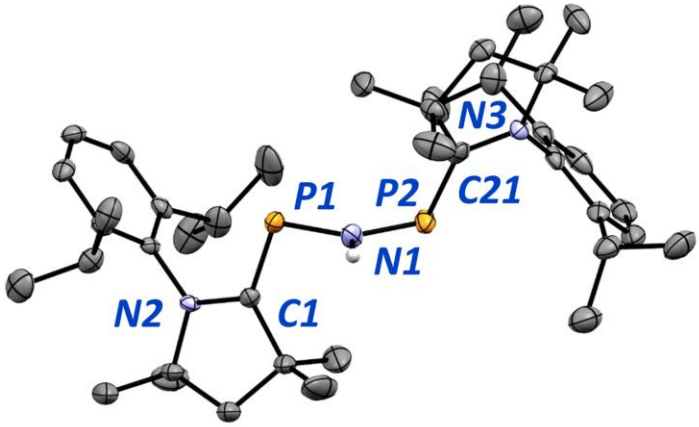

Figure 7. Molecular structure of **7**. Ellipsoids are drawn at 50% probability. Hydrogen atoms attached to carbon are omitted. Select bond lengths (Å) and angles (°) [calculated values in square brackets]: N1-P1 1.732(4) [1.718]; N1-P2 1.719(3) [1.718]; N1-H1 0.78(5) [1.007]; C1-P1 1.735(3) [1.723]; C21-P2 1.742(5) [1.723]; C1-N2 1.364(5) [1.360]; C21-N3 1.369(5) [1.360]; P1-N1-P2 123.6(2) [121.3]; P1-N1-H1 118(3) [119.4], P2-N1-H1 118(3) [119.4].

While both the apparent solution structure and protonation of **K6$_{sol}$** is consistent with the alkali metal amide formulation, its solid-state structure reveals this descriptor to belie the rich coordination available to anion [**6**]$^-$. Deep red crystals suitable for X-ray diffraction experiments could be grown from a toluene/n-hexane mixture, the analysis of which shows the solid-state structure to be neither a dimer with a bridging K_2N_2 core, nor a toluene solvate typical of bulky potassium amide species.[89-92] Instead, an asymmetric dimeric solvent free structure **K$_2$6$_2$** was obtained (Scheme 4, Figure 8) in which neither fragment binds to potassium in κ^1-N or μ^2-N fashion expected of bulky potassium amides. In **K$_2$6$_2$**, one fragment bridges two inequivalent potassium ions through the PNP core, binding to each in κ^1-P fashion, while the diisopropylphenyl fragments of both CAAC^{Me} ligands associate to both potassium ions through cation-π interactions. The other fragment associates with one potassium ion through the π-face of the PNP moiety in η^3-fashion, while the diisopropylphenyl group of one of the CAAC^{Me} ligands interacts with the other potassium ion through cation-π interactions. Dissolution of crystals of **K$_2$6$_2$** in C_6D_6 and analysis by $^{31}P\{^1H\}$ NMR spectroscopy showed resonances matching the spectrum of the symmetric species **K6$_{sol}$**, indicating that the dimeric structure is disassembled by interactions with the solvent.

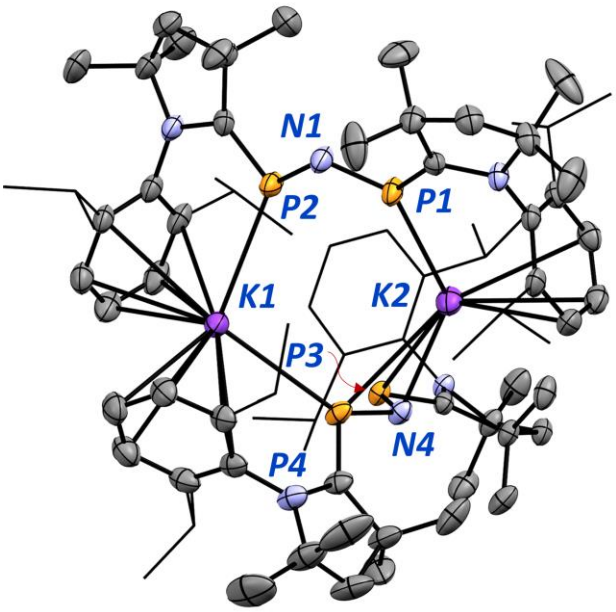

Figure 8. Molecular structure of **K$_2$6$_2$**. Ellipsoids are shown at 50% probability. Hydrogen atoms are omitted for clarity. Select bond lengths (Å) and angles (°) for **K$_2$6$_2$**: N1-P1 1.647(2); N1-P2 1.646(2); P1-K2 3.2395(9); P2-K1 3.215(1); C1-P1 1.702(3); C21-P2 1.705(3); N4-P3 1.677(2); N4-P4 1.670(2); N4-K2 2.760(2); P3-K2 3.5548(9); P4-K2 3.338(1); C41-P3 1.701(1); C61-P4 1.700(3); P1-N1-P2 115.2(1); P3-N4-P4 112.3(1).

To better examine the structure and bonding of free anion [**6**]$^-$ in the absence of potentially confounding influence from potassium ions, a freshly prepared THF solution of **K6$_{sol}$** was treated with [2.2.2]-cryptand that resulted in subtle darkening of the solution, from which charge-separated salt [K$_{crypt}$][**6**] could be isolated as red-orange crystalline needles after work-up (Scheme 4, Figure 9). [K$_{crypt}$][**6**] crystalizes with two sets of independent molecules per asymmetric unit, with the anionic fragments featuring similar bond lengths, differing mostly in the central PNP bond angle (119.1(3)° vs. 114.5(3)°). The geometry optimized structure of [**6**]$^-$ has a PNP bond angle of 116.7° (Figure 9), exactly in the middle of the two experimental angles, which suggests that the variance observed in the solid-state data can be attributed to packing effects.

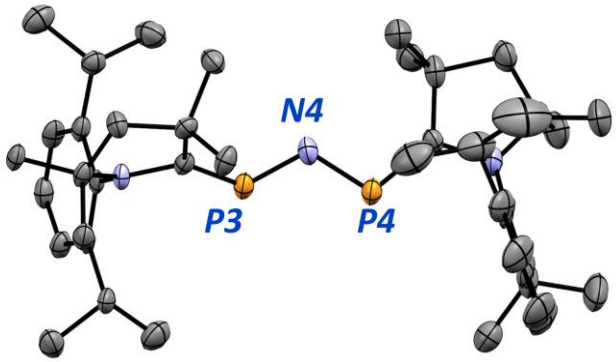

Figure 9. Molecular structure of [**6**]$^-$. Ellipsoids are shown at 50% probability. Only one crystallographically independent molecule of [**6**]$^-$ is shown. Hydrogen atoms are omitted for clarity. Select bond lengths (Å) and angles (°) [calculated values in square brackets]: N4-P3 1.674(4) [1.650]; N4-P4 1.641(5) [1.650]; P3-C41 1.699(4) [1.698]; P4-C61 1.707(5) [1.698]; P3-N4-P4 119.1(3) [116.7].

Curiously, despite the diamagnetic nature of **6**, the ^{1}H and ^{13}C NMR spectra of [K_{crypt}][**6**] contain only resonances attributable to the potassium-cryptate cation (Figure S16), while the $^{31}P\{^1H\}$ NMR spectrum shows a broad signal at 205.9 ppm ($\nu_{½}$ = 450 Hz, Figure S17), suggestive of paramagnetic character. In the solid state, [Kcrypt][**6**] is EPR silent, while in solution only the signal for **4** was detected, indicating facile reoxidation despite the use of rigorously purified solvents.

Conclusions

In summary, this work presents the first synthesis of a carbene-stabilized PNP radical, **4**, in a convenient one-pot procedure from free carbene and phosphazene salt [Cl_3PNPCl_3][Cl] by formal 7 e$^-$ reduction. The radical exhibits a delocalized electronic structure, with spin density distributed almost equally between the central nitrogen atom and the carbene ligands. Radical **4** was amenable to both one electron oxidation and reduction to formal nitrenium and amide species [**5**]$^+$ and [**6**]$^-$, respectively. [**5**]$^+$ exists in a dynamic equilibrium between the expected bent nitrenium structure [$\mathbf{5_b}$]$^+$ and a linear heteroallene like species [$\mathbf{5_a}$]$^+$, which has not been previously observed, and may have important implications for the growing field of cationic nitrogen chemistry. While displaying some chemistry typical of amides, such as nitrogen-centered protonation, the anion [**6**]$^-$ also exhibits exceptional flexibility in its coordination mode, suggestive of a potentially diverse

coordination chemistry, and may serve as convenient synthon for nucleophilic installation of a redox active fragment to inorganic and organic compounds. The sum of these findings shows that the bonding and structure of low-valent PNP species differ substantially from the previously reported all-nitrogen and all-phosphorus congeners, across multiple species and oxidation states, and suggests that other binary PN fragments may display unexpected properties and accordingly warrant further investigation.

ACKNOWLEDGMENT

I.M. thanks the Canadian government for a Canada 150 Research Chair, NSERC for a Discovery Grant, and the University of Victoria for start-up funds. E.L. thanks NSERC for a Post-doctoral Fellowship. H.M.T. thanks the University of Jyväskylä for financial support and acknowledges a grant of computing capacity from the Finnish Grid and Cloud Infrastructure (persistent identifier urn:nbn:fi:research-infras-2016072533). J.M.R. thanks NSERC for financial support through a Discovery operating grant (2020-04627).

REFERENCES

1. Danen, W. C.; Neugebauer, F. A., Aminyl Free-Radicals. *Angew. Chem. Int. Ed.* **1975,** *14* (12), 783-789.
2. Hicks, R. G., What's new in stable radical chemistry? *Org. Biomol. Chem.* **2007,** 5 (9), 1321-38.
3. Hioe, J.; Sakic, D.; Vrcek, V.; Zipse, H., The stability of nitrogen-centered radicals. *Org. Biomol. Chem.* **2015,** *13* (1), 157-69.
4. Stubbe, J.; van Der Donk, W. A., Protein Radicals in Enzyme Catalysis. *Chem. Rev.* **1998,** *98* (2), 705-762.
5. Zard, S. Z., Recent progress in the generation and use of nitrogen-centred radicals. *Chem. Soc. Rev.* **2008,** *37* (8), 1603-18.
6. Chen, J. R.; Hu, X. Q.; Lu, L. Q.; Xiao, W. J., Visible light photoredox-controlled reactions of N-radicals and radical ions. *Chem. Soc. Rev.* **2016,** *45* (8), 2044-56.
7. Xiong, T.; Zhang, Q., New amination strategies based on nitrogen-centered radical chemistry. *Chem. Soc. Rev.* **2016,** *45* (11), 3069-87.
8. Hawker, C. J., "Living" free radical polymerization: A unique technique for the preparation of controlled macromolecular architectures. *Acc. Chem. Res.* **1997,** *30* (9), 373-382.
9. Song, H.; Pietrasiak, E.; Lee, E., Persistent Radicals Derived from N-Heterocyclic Carbenes for Material Applications. *Acc. Chem. Res.* **2022,** 55 (16), 2213-2223.
10. Williams, D. E., Structure of 2,2-Diphenyl-1-picrylhydrazyl Free Radical1. *J. Am. Chem. Soc.* **1966,** *88* (23), 5665-5666.
11. Williams, D. E., Crystal Structure of 2,2-Diphenyl-1-Picrylhydrazyl Free Radical. *J. Am. Chem. Soc.* **1967,** *89* (17), 4280-&.
12. Miura, Y.; Tomimura, T.; Teki, Y., Heterocycle-substituted stable thioaminyl radicals: isolation, ESR spectra, and magnetic properties(1). *J. Org. Chem.* **2000,** *65* (23), 7889-95.
13. Miura, Y.; Tomimura, T., First isolation of N-alkoxyaminyl radicals. *Chem. Commun.* **2001,** (7), 627-628.
14. Buttner, T.; Geier, J.; Frison, G.; Harmer, J.; Calle, C.; Schweiger, A.; Schonberg, H.; Grutzmacher, H., A stable aminyl radical metal complex. *Science* **2005,** *307* (5707), 235-8.
15. Maire, P.; Konigsmann, M.; Sreekanth, A.; Harmer, J.; Schweiger, A.; Grutzmacher, H., A tetracoordinated rhodium aminyl radical complex. *J. Am. Chem. Soc.* **2006,** *128* (20), 6578-80.
16. Eymann, L. Y.; Tskhovrebov, A. G.; Sienkiewicz, A.; Bila, J. L.; Zivkovic, I.; Ronnow, H. M.; Wodrich, M. D.; Vannay, L.; Corminboeuf, C.; Pattison, P.; Solari, E.; Scopelliti, R.; Severin, K., Neutral Aminyl Radicals Derived from Azoimidazolium Dyes. *J. Am. Chem. Soc.* **2016,** *138* (46), 15126-15129.
17. Back, J.; Park, J.; Kim, Y.; Kang, H.; Kim, Y.; Park, M. J.; Kim, K.; Lee, E., Triazenyl Radicals Stabilized by N-Heterocyclic Carbenes. *J. Am. Chem. Soc.* **2017,** *139* (43), 15300-15303.
18. Shimizu, D.; Furukawa, K.; Osuka, A., Stable Subporphyrin meso-Aminyl Radicals without Resonance Stabilization by a Neighboring Heteroatom. *Angew. Chem. Int. Ed.* **2017,** *56* (26), 7435-7439.
19. Shimizu, D.; Fujimoto, K.; Osuka, A., Stable Diporphyrinylaminyl Radical and Nitrenium Ion. *Angew. Chem. Int. Ed.* **2018,** *57* (30), 9434-9438.

20. Kundu, S.; Sinhababu, S.; Chandrasekhar, V.; Roesky, H. W., Stable cyclic (alkyl)(amino)carbene (cAAC) radicals with main group substituents. *Chem. Sci,* **2019,** *10* (18), 4727-4741.
21. Soleilhavoup, M.; Bertrand, G., Cyclic (alkyl)(amino)carbenes (CAACs): stable carbenes on the rise. *Acc. Chem. Res.* **2015,** *48* (2), 256-66.
22. Melaimi, M.; Jazzar, R.; Soleilhavoup, M.; Bertrand, G., Cyclic (Alkyl)(amino)carbenes (CAACs): Recent Developments. *Angew. Chem. Int. Ed.* **2017,** *56* (34), 10046-10068.
23. Nesterov, V.; Reiter, D.; Bag, P.; Frisch, P.; Holzner, R.; Porzelt, A.; Inoue, S., NHCs in Main Group Chemistry. *Chem. Rev.* **2018,** *118* (19), 9678-9842.
24. Matyáš, R.; Pachman, J., Nitrogen Halides. In *Primary Explosives*, Matyáš, R.; Pachman, J., Eds. Springer Berlin Heidelberg: Berlin, Heidelberg, 2013; pp 289-302.
25. Back, J.; Kwon, G.; Byeon, J. E.; Song, H.; Kang, K.; Lee, E., Tunable Redox-Active Triazenyl-Carbene Platforms: A New Class of Anolytes for Non-Aqueous Organic Redox Flow Batteries. *ACS Appl Mater Interfaces* **2020,** *12* (33), 37338-37345.
26. Kim, Y.; Kim, K.; Lee, E., Oxime Ether Radical Cations Stabilized by N-Heterocyclic Carbenes. *Angew. Chem. Int. Ed.* **2018,** 57 (1), 262-265.
27. Kim, Y.; Lee, E., Stable Organic Radicals Derived from N-Heterocyclic Carbenes. *Chem. Eur. J.* **2018,** *24* (72), 19110-19121.
28. Park, J.; Song, H.; Kim, Y.; Eun, B.; Kim, Y.; Bae, D. Y.; Park, S.; Rhee, Y. M.; Kim, W. J.; Kim, K.; Lee, E., N-heterocyclic carbene nitric oxide radicals. *J. Am. Chem. Soc.* **2015,** *137* (14), 4642-5.
29. Kinjo, R.; Donnadieu, B.; Bertrand, G., Isolation of a carbene-stabilized phosphorus mononitride and its radical cation (PN+*). *Angew. Chem. Int. Ed.* **2010,** *49* (34), 5930-3.
30. Back, O.; Donnadieu, B.; von Hopffgarten, M.; Klein, S.; Tonner, R.; Frenking, G.; Bertrand, G., N-Heterocyclic carbenes versus transition metals for stabilizing phosphinyl radicals. *Chem. Sci.* **2011,** *2* (5), 858-861.
31. Tondreau, A. M.; Benkő, Z.; Harmer, J. R.; Grützmacher, H., Sodium phosphaethynolate, Na(OCP), as a "P" transfer reagent for the synthesis of N-heterocyclic carbene supported P3and PAsP radicals. *Chem. Sci.* **2014,** 5 (4), 1545-1554.
32. Back, O.; Celik, M. A.; Frenking, G.; Melaimi, M.; Donnadieu, B.; Bertrand, G., A crystalline phosphinyl radical cation. *J. Am. Chem. Soc.* **2010,** *132* (30), 10262-3.
33. Rivard, E.; Lough, A. J.; Manners, I., A new, convenient synthesis of the linear phosphazene salt [Cl3P=N=PCl3]Cl: preparation of higher linear homologues [Cl3P=N-(PCl2=N)x=PCl3]Cl (x = 1-3) and the 16-membered macrocycle [NCCl(NPCl2)3]2. *Inorg. Chem.* **2004,** *43* (9), 2765-7.
34. Fluck, E.; Schmid, E.; Haubold, W., Notizen: 2.2.4.4.6-Pentachlor-2.4-diphospha-1.3.5-striazin / 2,2,4,4,6-Pentachloro-2,4-diphospha-1,3,5-s-triazine. *Zeitschrift für Naturforschung B* **1975,** *30* (9-10), 808-809.
35. Becke-Goehring, M.; Lehr, W., Über Phosphorstickstoffverbindungen. XIV. Die Verbindungen mit der Zusammensetzung P2NCl7. *Z. Anorg. Allg. Chem.* **1963,** *325* (5-6), 287-301.
36. Wang, B.; Rivard, E.; Manners, I., A new high-yield synthesis of Cl(3)P=NSiMe(3), a monomeric precursor for the controlled preparation of high molecular weight polyphosphazenes. *Inorg. Chem.* **2002,** *41* (7), 1690-1.
37. Manners, I.; Allcock, H. R.; Renner, G.; Nuyken, O., Poly(Carbophosphazenes) - a New Class of Inorganic-Organic Macromolecules. *J. Am. Chem. Soc.* **1989,** *111* (14), 5478-5480.
38. Dodge, J. A.; Manners, I.; Allcock, H. R.; Renner, G.; Nuyken, O., Poly(Thiophosphazenes) - New Inorganic Macromolecules with Backbones Composed of Phosphorus, Nitrogen, and Sulfur-Atoms. *J. Am. Chem. Soc.* **1990,** *112* (3), 1268-1269.
39. Blackstone, V.; Pfirrmann, S.; Helten, H.; Staubitz, A.; Presa Soto, A.; Whittell, G. R.; Manners, I., A cooperative role for the counteranion in the PCl5-initiated living, cationic chain growth polycondensation of the phosphoranimine Cl3P =NSiMe3. *J. Am. Chem. Soc.* **2012,** *134* (37), 15293-6.
40. Blackstone, V.; Lough, A. J.; Murray, M.; Manners, I., Probing the mechanism of the PCl5-initiated living cationic polymerization of the phosphoranimine Cl3P=NSiMe3 using model compound chemistry. *J. Am. Chem. Soc.* **2009,** *131* (10), 3658-67.
41. Suárez Suárez, S.; Presa Soto, D.; Carriedo, G. A.; Presa Soto, A.; Staubitz, A., Experimental and Theoretical Study of the Living Polymerization of N-Silylphosphoranimines. Synthesis of New Block Copolyphosphazenes. *Organometallics* **2012,** *31* (7), 2571-2581.
42. Fluck, E.; Hsle, R., Trichlorphosphazophosphordichlorid, Cl3P=N-PCl2. *Z. Anorg. Allg. Chem.* **1979,** *458* (1), 103-107.
43. Velian, A.; Cummins, C. C., Inorganic chemistry. Synthesis and characterization of P(2)N(3)(-): an aromatic ion composed of phosphorus and nitrogen. *Science* **2015,** *348* (6238), 1001-4.
44. Zhu, C.; Eckhardt, A. K.; Bergantini, A.; Singh, S. K.; Schreiner, P. R.; Kaiser, R. I., The elusive cyclotriphosphazene molecule and its Dewar benzene-type valence isomer (P(3)N(3)). *Sci Adv* **2020,** *6* (30), eaba6934.
45. Roesky, H. W., Preparation of Hexaazidophosphates. *Angew. Chem. Int. Ed.* **1967,** *6* (7), 637-&.

46. Buder, W.; Schmidt, A., Phosphorazide und deren Schwingungsspektren. *Z. Anorg. Allg. Chem.* **1975,** *415* (3), 263-267.
47. Volgnandt, P.; Schmidt, A., Natrium- und Tetraalkylammonium-hexaazidophosphate. Darstellung und Schwingungsspektren. Berichtigung zur Arbeit: Phosphorazide und deren Schwingungsspektren [1]. *Z. Anorg. Allg. Chem.* **1976,** *425* (2), 189-192.
48. Haiges, R.; Schneider, S.; Schroer, T.; Christe, K. O., High-energy-density materials: synthesis and characterization of N5+[P(N3)6]-, N5+[B(N3)4]-, N5+[HF2]-.n HF, N5+[BF4]-, N5+[PF6]-, and N5+[SO3F]. *Angew. Chem. Int. Ed.* **2004,** *43* (37), 4919-24.
49. Gobel, M.; Karaghiosoff, K.; Klapotke, T. M., The first structural characterization of a binary P-N molecule: the highly energetic compound P3N21. *Angew. Chem. Int. Ed.* **2006,** *45* (36), 6037-40.
50. Turner, B. E.; Bally, J., Detection of interstellar PN - The first identified phosphorus compound in the interstellar medium. *The Astrophysical Journal* **1987,** *321*, L75.
51. Tofan, D.; Velian, A., Interstellar Chemistry in a Glovebox: Elusive Diatomic P≡N, Exposed. *ACS Cent Sci* **2020,** *6* (9), 1485-1487.
52. Martinez, J. L.; Lutz, S. A.; Beagan, D. M.; Gao, X.; Pink, M.; Chen, C. H.; Carta, V.; Moenne-Loccoz, P.; Smith, J. M., Stabilization of the Dinitrogen Analogue, Phosphorus Nitride. *ACS Cent Sci* **2020,** *6* (9), 1572-1577.
53. Eckhardt, A. K.; Riu, M. Y.; Ye, M.; Muller, P.; Bistoni, G.; Cummins, C. C., Taming phosphorus mononitride. *Nat Chem* **2022,** *14* (8), 928-934.
54. Back, O.; Kuchenbeiser, G.; Donnadieu, B.; Bertrand, G., Nonmetal-mediated fragmentation of P4: isolation of P1 and P2 bis(carbene) adducts. *Angew. Chem. Int. Ed.* **2009,** *48* (30), 5530-3.
55. Back, O.; Donnadieu, B.; Parameswaran, P.; Frenking, G.; Bertrand, G., Isolation of crystalline carbene-stabilized P(2)-radical cations and P(2)-dications. *Nat Chem* **2010,** *2* (5), 369-73.
56. Back, O.; Henry-Ellinger, M.; Martin, C. D.; Martin, D.; Bertrand, G., 31P NMR chemical shifts of carbene-phosphinidene adducts as an indicator of the pi-accepting properties of carbenes. *Angew. Chem. Int. Ed.* **2013,** *52* (10), 2939-43.
57. Wang, Y.; Xie, Y.; Wei, P.; King, R. B.; Schaefer, H. F., 3rd; Schleyer, P.; Robinson, G. H., Carbene-stabilized diphosphorus. *J. Am. Chem. Soc.* **2008,** *130* (45), 14970-1.
58. Ellis, B. D.; Dyker, C. A.; Decken, A.; Macdonald, C. L., The synthesis, characterisation and electronic structure of N-heterocyclic carbene adducts of P(I) cations. *Chem. Commun.* **2005,** (15), 1965-7.
59. Roy, S.; Mondal, K. C.; Kundu, S.; Li, B.; Schurmann, C. J.; Dutta, S.; Koley, D.; Herbst-Irmer, R.; Stalke, D.; Roesky, H. W., Two Structurally Characterized Conformational Isomers with Different C-P Bonds. *Chem. Eur. J.* **2017,** *23* (50), 12153-12157.
60. Sharma, M. K.; Blomeyer, S.; Glodde, T.; Neumann, B.; Stammler, H. G.; Hinz, A.; van Gastel, M.; Ghadwal, R. S., Isolation of singlet carbene derived 2-phospha-1,3-butadienes and their sequential one-electron oxidation to radical cations and dications. *Chem. Sci,* **2020,** *11* (7), 1975-1984.
61. Liu, L. L.; Ruiz, D. A.; Dahcheh, F.; Bertrand, G., Isolation of a Lewis base stabilized parent phosphenium (PH2(+)) and related species. *Chem. Commun.* **2015,** *51* (64), 12732-12735.
62. Kulkarni, A.; Arumugam, S.; Francis, M.; Reddy, P. G.; Nag, E.; Gorantla, S.; Mondal, K. C.; Roy, S., Solid-State Isolation of Cyclic Alkyl(Amino) Carbene (cAAC)-Supported Structurally Diverse Alkali Metal-Phosphinidenides. *Chem. Eur. J.* **2021,** *27* (1), 200-206.
63. Niecke, E.; Bitter, W., N-Trimethylsilyl-Trichlorphosphinimin. *Inorganic & Nuclear Chemistry Letters* **1973,** *9* (2), 127-129.
64. Huynh, K.; Rivard, E.; Leblanc, W.; Blackstone, V.; Lough, A. J.; Manners, I., Phosphine-mediated dehalogenation reactions of trichloro(N-silyl)phosphoranimines. *Inorg. Chem.* **2006,** *45* (19), 7922-8.
65. Rivard, E.; Huynh, K.; Lough, A. J.; Manners, I., Donor-stabilized cations and imine transfer from N-silylphosphoranimines. *J. Am. Chem. Soc.* **2004,** *126* (8), 2286-7.
66. Lewis, G. R.; Dance, I., Crystal supramolecularity. Multiple phenyl embraces by [PPN](+) cations. *Journal of the Chemical Society-Dalton Transactions* **2000,** (3), 299-306.
67. Burford, N.; Cameron, T. S.; LeBlanc, D. J.; Phillips, A. D.; Concolino, T. E.; Lam, K. C.; Rheingold, A. L., Iminophosphide bonding environments from carbene complexes of iminophosphines. *J. Am. Chem. Soc.* **2000,** *122* (22), 5413-5414.
68. Burford, N.; Losier, P.; Phillips, A. D.; Ragogna, P. J.; Cameron, T. S., Nitrogen ligands on phosphorus(III) Lewis acceptors: A versatile new synthetic approach to unusual N-P structural arrangements. *Inorg. Chem.* **2003,** *42* (4), 1087-91.
69. Pyykko, P., Additive covalent radii for single-, double-, and triple-bonded molecules and tetrahedrally bonded crystals: a summary. *J. Phys. Chem. A* **2015,** *119* (11), 2326-37.
70. Romanov, A. S.; Bochmann, M., Gold(I) and Gold(III) Complexes of Cyclic (Alkyl)(amino)carbenes. *Organometallics* **2015,** *34* (11), 2439-2454.

71. Saito, T.; Nishiyama, H.; Tanahashi, H.; Kawakita, K.; Tsurugi, H.; Mashima, K., 1,4-Bis(trimethylsilyl)-1,4-diaza-2,5-cyclohexadienes as strong salt-free reductants for generating low-valent early transition metals with electron-donating ligands. *J. Am. Chem. Soc.* **2014,** *136* (13), 5161-70.
72. Tsurugi, H.; Mashima, K., Salt-Free Reduction of Transition Metal Complexes by Bis(trimethylsilyl)cyclohexadiene, -dihydropyrazine, and -4,4'-bipyridinylidene Derivatives. *Acc. Chem. Res.* **2019,** *52* (3), 769-779.
73. Kaim, W., Effects of cyclic 8π-electron conjugation in reductively silylated nitrogen heterocycles. *J. Am. Chem. Soc.* **2002,** *105* (4), 707-713.
74. Schubert, E. M., Utilizing the Evans Method with a Superconducting Nmr Spectrometer in the Undergraduate Laboratory. *J. Chem. Educ.* **1992,** *69* (1), 62-62.
75. Bordwell, F. G.; Cheng, J.; Ji, G. Z.; Satish, A. V.; Zhang, X., Bond dissociation energies in DMSO related to the gas phase values. *J. Am. Chem. Soc.* **2002,** *113* (26), 9790-9795.
76. Laarhoven, L. J. J.; Mulder, P.; Wayner, D. D. M., Determination of bond dissociation enthalpies in solution by photoacoustic calorimetry. *Acc. Chem. Res.* **1999,** *32* (4), 342-349.
77. Tulchinsky, Y.; Iron, M. A.; Botoshansky, M.; Gandelman, M., Nitrenium ions as ligands for transition metals. *Nat Chem* **2011,** *3* (7), 525-31.
78. Tulchinsky, Y.; Kozuch, S.; Saha, P.; Mauda, A.; Nisnevich, G.; Botoshansky, M.; Shimon, L. J.; Gandelman, M., Coordination chemistry of N-heterocyclic nitrenium-based ligands. *Chem. Eur. J.* **2015,** *21* (19), 7099-110.
79. Zhou, J.; Liu, L. L.; Cao, L. L.; Stephan, D. W., Nitrogen-Based Lewis Acids: Synthesis and Reactivity of a Cyclic (Alkyl)(Amino)Nitrenium Cation. *Angew. Chem. Int. Ed.* **2018,** *57* (13), 3322-3326.
80. Mehta, M.; Goicoechea, J. M., Nitrenium Salts in Lewis Acid Catalysis. *Angew. Chem. Int. Ed.* **2020,** *59* (7), 2715-2719.
81. Zhu, D.; Qu, Z. W.; Zhou, J.; Stephan, D. W., The Reactivity of Isomeric Nitrenium Lewis Acids with Phosphines, Carbenes, and Phosphide. *Chem. Eur. J.* **2021,** *27* (8), 2861-2867.
82. Pogoreltsev, A.; Tulchinsky, Y.; Fridman, N.; Gandelman, M., Nitrogen Lewis Acids. *J. Am. Chem. Soc.* **2017,** *139* (11), 4062-4067.
83. Waked, A. E.; Ostadsharif Memar, R.; Stephan, D. W., Nitrogen-Based Lewis Acids Derived from Phosphonium Diazo Cations. *Angew. Chem. Int. Ed.* **2018,** *57* (37), 11934-11938.
84. Bates, R.; Macaskill, J., Standard potential of the silver-silver chloride electrode. *Pure Appl. Chem* **1978,** *50* (11-12), 1701-1706.
85. Elgrishi, N.; Rountree, K. J.; McCarthy, B. D.; Rountree, E. S.; Eisenhart, T. T.; Dempsey, J. L., A Practical Beginner's Guide to Cyclic Voltammetry. *J. Chem. Educ.* **2018,** *95* (2), 197-206.
86. Aranzaes, J. R.; Daniel, M. C.; Astruc, D., Metallocenes as references for the determination of redox potentials by cyclic voltammetry - Permethylated iron and cobalt sandwich complexes, inhibition by polyamine dendrimers, and the role of hydroxy-containing ferrocenes. *Can. J. Chem.* **2006,** *84* (2), 288-299.
87. Winkelhaus, D.; Holthausen, M. H.; Dobrovetsky, R.; Stephan, D. W., Phosphine and carbene azido-cations: [(L)N(3)](+) and [(L)(2)N(3)]+. *Chem. Sci,* **2015,** *6* (11), 6367-6372.
88. Neufeld, R.; Stalke, D., Accurate molecular weight determination of small molecules via DOSY-NMR by using external calibration curves with normalized diffusion coefficients. *Chem. Sci,* **2015,** *6* (6), 3354-3364.
89. Nicholas, H. M.; Goodwin, C. A. P.; Kragskow, J. G. C.; Lockyer, S. J.; Mills, D. P., Structural Characterization of Lithium and Sodium Bulky Bis(silyl)amide Complexes. *Molecules* **2018,** *23* (5), 1138.
90. Kays, D. L., Extremely bulky amide ligands in main group chemistry. *Chem. Soc. Rev.* **2016,** *45* (4), 1004-18.
91. Coombs, N. D.; Stasch, A.; Cowley, A.; Thompson, A. L.; Aldridge, S., Bulky aryl functionalized carbazolyl ligands: amido alternatives to the 2,6-diarylphenyl ligand class? *Dalton Trans.* **2008,** (3), 332-7.
92. Goodwin, C. A. P.; Joslin, K. C.; Lockyer, S. J.; Formanuik, A.; Morris, G. A.; Ortu, F.; Vitorica-Yrezabal, I. J.; Mills, D. P., Homoleptic Trigonal Planar Lanthanide Complexes Stabilized by Superbulky Silylamide Ligands. *Organometallics* **2015,** *34* (11), 2314-2325.